Design principles of the proteolytic cascade governing the σ^E-mediated envelope stress response in *Escherichia coli*: keys to graded, buffered, and rapid signal transduction

Rachna Chaba,[1,6] Irina L. Grigorova,[2,6,7] Julia M. Flynn,[4,5] Tania A. Baker,[4,5] and Carol A. Gross[1,3,8]

[1]Department of Microbiology and Immunology, University of California at San Francisco, San Francisco, California 94158, USA; [2]Graduate Group in Biophysics, University of California at San Francisco, San Francisco, California 94158, USA; [3]Department of Cell and Tissue Biology, University of California at San Francisco, San Francisco, California 94158, USA; [4]Department of Biology, Massachusetts Institute of Technology, Cambridge, Massachusetts 02139, USA; [5]Howard Hughes Medical Institute, Massachusetts Institute of Technology, Cambridge, Massachusetts 02139, USA

Proteolytic cascades often transduce signals between cellular compartments, but the features of these cascades that permit efficient conversion of a biological signal into a transcriptional output are not well elucidated. σ^E mediates an envelope stress response in *Escherichia coli*, and its activity is controlled by regulated degradation of RseA, a membrane-spanning anti-σ factor. Examination of the individual steps in this protease cascade reveals that the initial, signal-sensing cleavage step is rate-limiting; that multiple ATP-dependent proteases degrade the cytoplasmic fragment of RseA and that dissociation of σ^E from RseA is so slow that most free σ^E must be generated by the active degradation of RseA. As a consequence, the degradation rate of RseA is set by the amount of inducing signal, and insulated from the "load" on and activity of the cytoplasmic proteases. Additionally, changes in RseA degradation rate are rapidly reflected in altered σ^E activity. These design features are attractive as general components of signal transduction pathways governed by unstable negative regulators.

[*Keywords*: σ^E; stress response; proteolysis; ATP-dependent proteases; DegS; RseP]

Received September 25, 2006; revised version accepted November 7, 2006.

Proteolytic cascades are widely used to transduce signals across membranes to enable cells to respond to environmental stress and coordinate processes in different cellular compartments. However, the molecular properties of these cascades that facilitate the desired outputs have rarely been examined. In this work, we examine the individual steps in the protease cascade governing the activity of the σ^E-mediated envelope stress response in *Escherichia coli* to determine the construction features of this cascade that facilitate faithful transmission of signal and a rapid output.

σ^E directs RNA polymerase to transcribe genes encoding proteins that ensure the synthesis, assembly, and homeostasis of outer membrane porins and lipopolysaccharide, the two major components of the unique outer membrane of Gram-negative bacteria (Dartigalongue et al. 2001; Rezuchova et al. 2003; Rhodius et al. 2006). Envelope integrity is required under all growth conditions, and σ^E is an essential transcription factor (De Las Penas et al. 1997a). Perturbations in the integrity and protein-folding state of the envelope caused by temperature upshift, chaperone depletion, or accumulation of unassembled porins increase σ^E activity; conversely, temperature downshift and/or depletion of porins decrease σ^E activity (Mecsas et al. 1993; Hiratsu et al. 1995; Raina et al. 1995; Rouviere et al. 1995; Missiakas et al. 1996; Rouviere and Gross 1996; Ades et al. 2003).

The components of the signal transduction system that control σ^E activity are shown in Figure 1. RseA, a membrane-spanning anti-σ factor, inhibits σ^E activity. The cytoplasmic domain of RseA (RseA$^{1-108}$) binds to σ^E and its periplasmic domain binds to RseB (De Las Penas et al. 1997b; Missiakas et al. 1997). Interaction of σ^E with RseA prevents σ^E from binding to RNA polymerase (Campbell et al. 2003). This inhibitory interaction is re-

[6]These authors contributed equally to this work.
[7]Present address: Department of Microbiology and Immunology, University of California at San Francisco, 513 Parnassus Avenue, San Francisco, CA 94143, USA
[8]Corresponding author.
E-MAIL cgross@cgl.ucsf.edu; FAX (415) 514-4080.
Article is online at http://www.genesdev.org/cgi/doi/10.1101/gad.1496707.

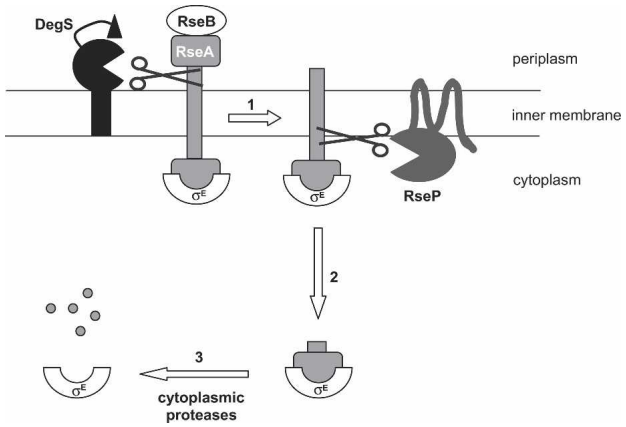

Figure 1. A protease cascade degrades RseA to release σ^E.

lieved when RseA is degraded via a proteolytic cascade. RseA is cleaved first in its periplasmic domain by DegS and then within its transmembrane region by the RIP protease, RseP, thereby releasing $RseA^{1-108}$ still bound to σ^E (Ades et al. 1999; Alba et al. 2002; Kanehara et al. 2002; Walsh et al. 2003; Akiyama et al. 2004). σ^E is finally released from this inhibitory interaction when $RseA^{1-108}$ is degraded by cytoplasmic proteases (Flynn et al. 2004).

The proteolytic cascade degrading RseA is activated by unassembled porins in the envelope compartment of the cell. Porins constitute 2% of all cellular proteins and form trimeric pores in the outer membrane (Nikaido 1996). When folding is inefficient, unassembled porins accumulate and their C termini activate DegS to initiate cleavage of RseA (Walsh et al. 2003). Exposed C termini are an excellent indicator of impaired folding as they are normally sequestered in the porin trimer interface (Cowan et al. 1995). Free DegS is inactive in cleaving RseA because its catalytic triad is inappropriately positioned. However, when porin C termini bind to the DegS PDZ domain, the catalytic triad is repositioned and cleavage of RseA ensues (Walsh et al. 2003; Wilken et al. 2004). DegS, RseB, RseA, and the PDZ domain of RseP itself all inhibit RseP cleavage of intact RseA, thereby ensuring that DegS always acts before RseP in the RseA-processing pathway (Kanehara et al. 2003; Bohn et al. 2004; Grigorova et al. 2004). Since DegS is the only protease that senses the porin signal, obligate sequential cleavage of RseA ensures that the initiation of the proteolytic cascade reflects the status of this inducing signal.

In the present study we dissect the individual steps in the proteolytic cascade degrading RseA. A kinetic description of the pathway reveals that the initial signal-sensing cleavage step is rate-limiting under all conditions, ensuring that the overall degradation rate of RseA reflects signal status. We find that RseA and σ^E interact with picomolar affinity, ensuring that free σ^E is generated almost exclusively by cytoplasmic ATP-dependent proteases that disassemble the complex and degrade $RseA^{1-108}$. Indeed, enormous resources are invested into clearing $RseA^{1-108}$ from the cell: Essentially, the entire network of cytoplasmic ATP-dependent proteases participates in this process. We will discuss why the organizational structure of this protease cascade facilitates rapid and sensitive transmission of signal to the output response. Proteolytic cascades govern a variety of processes in diverse organisms (Brown et al. 2000; Weihofen and Martoglio 2003). We believe that the investigation and subsequent cross-comparison of such pathways will significantly improve our understanding of the principles that underlie these signaling proteolytic cascades.

Results

A kinetic description of the degradation of RseA under inducing conditions

Initiation of RseA degradation by DegS is relatively slow during steady-state growth ($T_{1/2} \sim 8$ min) (Ades et al. 2003), and is rate-limiting under these noninducing conditions, as no intermediates in degradation were observed (Ades et al. 1999; Alba et al. 2002; Kanehara et al. 2002; Akiyama et al. 2004). Here, we determined whether initiation of RseA degradation is rate-limiting when stress is generated by overexpressing the YYF peptide (Walsh et al. 2003). We measured the $T_{1/2}$ of all three RseA species (full-length RseA, DegS cleavage product, and RseP cleavage product) using the pulse-chase protocol described in Ades et al. (2003) that is known not to disrupt the physiological state of the cells (see Materials and Methods).

A typical gel showing pulse chase data for degradation of RseA under inducing conditions is shown in Figure 2A. Quantification of the disappearance of full-length RseA (Fig. 1, Step 1) reveals that cleavage by DegS is initiated with a $T_{1/2}$ of 1 min (Fig. 2B). An intermediate-sized band (termed RseA-I) (Fig. 2A), corresponds to the initial DegS cleavage product: It is identical in size to the RseA product generated in a strain unable to process DegS cleaved RseA further because it lacks RseP (data not shown). The level of RseA-I reflects both its rate of generation by DegS cleavage and its rate of disappearance as a consequence of cleavage by RseP (Fig. 1, Step 2). Knowing the rate of DegS cleavage, we were able to calculate that this intermediate has a $T_{1/2} \leq 20$ sec, which reflects the rate of RseP cleavage (see Materials and Methods). Although a faint band corresponding to the cytoplasmic fragment of RseA ($RseA^{1-108}$ generated by RseP cleavage) is visible on the gel, it was too weak to be quantified. Therefore, we isolated this step from the circuitry of the σ^E signal transduction pathway and then measured the degradation rate of $RseA^{1-108}$ when in complex with σ^E (Fig. 1, Step 3). To do this, adjacent plasmid-located genes encoding $RseA^{1-108}$ and σ^E were expressed from a modified (trc) promoter with low activity (see Materials and Methods). We estimate that each protein was overexpressed ~10-fold (R. Chaba, unpubl.; see Materials and Methods). Under these conditions, the steady-state level of $RseA^{1-108}$ is barely visible on a Western blot; however, disappearance of this pro-

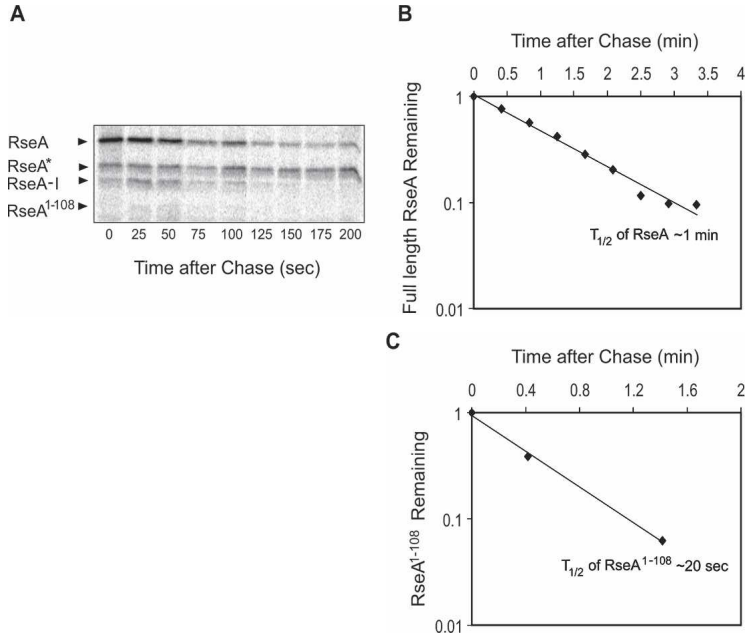

Figure 2. Cleavage of RseA by DegS is rate-limiting under inducing conditions. (*A*) Degradation of RseA in wild-type cells after initiation of the stress response by overexpression of YYF peptide. CAG53077 was grown in supplemented M9 media at 30°C to O.D.$_{450}$ ~ 0.15, and the stress response was initiated by the addition of IPTG to induce expression of YYF peptide. After 10 min of induction, the cells were pulse-labeled with L-[^{35}S] methionine, followed by a chase of unlabeled methionine. At various time points after the chase, cells were collected and processed as described in Materials and Methods. Bands corresponding to the full-length RseA (RseA), RseA intermediate generated by cleavage of RseA by DegS (RseA-I), cytoplasmic fragment of RseA generated upon cleavage by RseP (RseA$^{1–108}$), and the standard (RseA*; see Materials and Methods) are indicated by arrows. (*B*) Cleavage of full-length RseA by DegS. The rate of cleavage of full-length RseA by DegS under inducing conditions was determined by measuring the $T_{1/2}$ of RseA in wild-type cells (CAG53077) upon overexpression of YYF peptide as described in Materials and Methods. A representative data set is shown. (*C*) The stability of RseA$^{1–108}$ in wild-type cells. CAG53209 was grown in supplemented M9 media at 30°C to O.D.$_{450}$ ~ 0.2, and induced with IPTG for 10 min to overexpress RseA$^{1–108}$/σ^{E}. The stability of RseA$^{1–108}$ was determined as described in Materials and Methods. A representative data set is shown.

tein could be reproducibly quantified using a pulse-chase protocol. These experiments revealed that the rate of degradation of RseA$^{1–108}$ was very rapid ($T_{1/2} \leq 20$ sec, Fig. 2C; Fig. 1, Step 3). Thus, we conclude that cleavage by DegS is the slowest step in the RseA degradation pathway under inducing conditions.

The cytoplasmic domain of RseA binds very tightly to σ^{E}

In principle, σ^{E} could be released from RseA$^{1–108}$ both by dissociation and by degradation. To investigate the relative contributions of these two processes, we characterized the stability of the complex using RseA$^{1–100}$, a slightly truncated version of the normal cytoplasmic fragment (RseA$^{1–108}$). This fragment is easy to purify because it is stable in *E. coli*. It is also sufficient for anti-σ activity both in vivo and in vitro (De Las Penas et al. 1997b; Missiakas et al. 1997; Campbell et al. 2003). We used fluorescence anisotropy to measure the dissociation of rhodamine-labeled RseA$^{1–100}$ from σ^{E}. To permit rhodamine labeling, residue E28 was mutated to cysteine, chosen because it was far from the RseA–σ^{E} interface. The anisotropy of rhodamine-labeled RseA$^{1–100}$E28C was considerably lower than that of the labeled RseA$^{1–100}$E28C/σ^{E} complex (Fig. 3A). Therefore dissociation of labeled RseA$^{1–100}$E28C from σ^{E} in the presence of excess unlabeled RseA can be measured by determining the kinetics of the decrease in anisotropy. These experiments revealed that in the presence of a 10-fold excess of unlabeled RseA$^{1–100}$ there was no decrease in anisotropy during a 2-h time course, indicating that the dissociation rate constant of RseA$^{1–100}$E28C from σ^{E} was much less than 10^{-4} sec^{-1} (Fig. 3B). This very slow dissociation rate is not an artifact of the E28C substitution and/or rhodamine labeling since equivalent results were obtained from the reverse experiment: A 10-fold excess of rhodamine-labeled RseA$^{1–100}$E28C did not compete for unlabeled RseA$^{1–100}$ bound to authentic σ^{E} during 2 h of incubation (data not shown). These experiments indicate that the RseA$^{1–100}$/σ^{E} complex dissociates very slowly in vitro.

To measure the association rate constant between rhodamine-labeled RseA$^{1–100}$E28C and σ^{E}, we followed changes in fluorescence intensity after mixing reactants in a stopped-flow apparatus (Fig. 3C). The determined value of $1.5 \pm 0.2 \times 10^{7}$ M^{-1} sec^{-1} is close to that expected for a diffusion-limited reaction. This rate constant is neither a consequence of the E28C substitution nor of the labeling: Binding of both unlabeled RseA$^{1–100}$ and labeled RseA$^{1–100}$E28C to σ^{E} was confirmed to be the same by measuring changes in anisotropy induced by addition of σ^{E} to labeled RseA$^{1–100}$E28C premixed at different concentrations with unlabeled RseA$^{1–100}$ (data not shown). Based on the measured values of the association and dissociation rate constants, the equilibrium dissociation constant (K_d) between RseA$^{1–100}$ and σ^{E} in vitro is very tight (<10 pM). Taken together, the rapid degradation of RseA$^{1–108}$ (Fig. 2C) compared with the very slow spontaneous dissociation of σ^{E} from RseA$^{1–100}$ strongly suggests that free σ^{E} is predominantly generated by the ATP-dependent, enzyme-catalyzed process of RseA degradation in vivo.

Multiple ATP-dependent proteases degrade RseA$^{1–108}$ in vitro

The ATP-dependent unfoldase/protease ClpXP is competent both to disassemble the RseA$^{1–108}$/σ^{E} complex

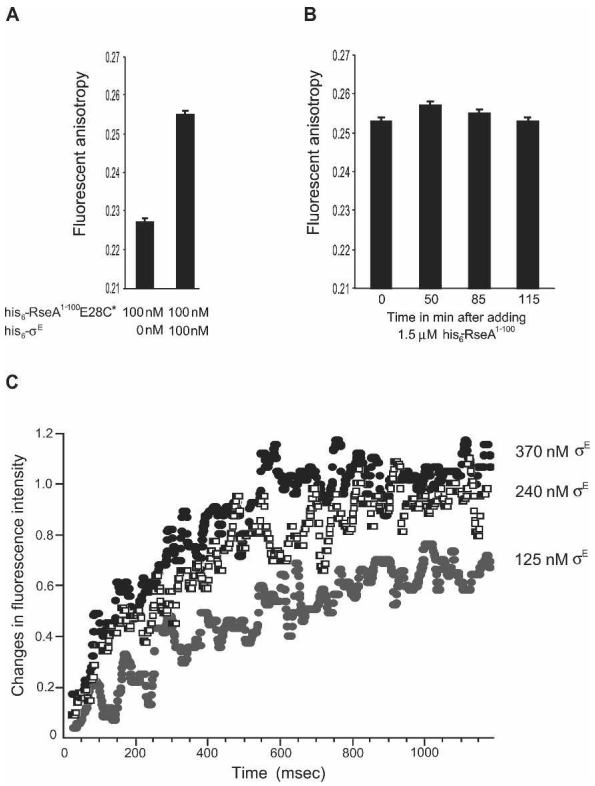

Figure 3. Kinetic measurements of the dissociation and association rate constants of σ^E binding to $RseA^{1–100}$. (*A*) Fluorescent anisotropy of rhodamine-labeled his_6-$RseA^{1–100}$E28C (his_6-$RseA^{1–100}$E28C*) alone and in complex with his_6-σ^E. (*B*) Changes in fluorescent anisotropy of the complex between his_6-$RseA^{1–100}$E28C* and his_6-σ^E (100 nM) after the addition of excess unlabeled his_6-$RseA^{1–100}$ (1.5 μM). (*C*) Changes in fluorescence intensity of his_6-$RseA^{1–100}$E28C*, induced by binding of his_6-σ^E. his_6-$RseA^{1–100}$E28C* (128 nM) was rapidly mixed with various concentrations of his_6-σ^E (125, 240, and 370 nM), using a stopped flow technique.

and to degrade $RseA^{1–108}$; $RseA^{1–108}$ alone and in complex with σ^E were degraded at approximately equivalent rates (Flynn et al. 2004). We determined whether any other ATP-dependent proteases could perform these reactions in vitro. Except for HslUV, all of the ATP-dependent proteases degraded free $RseA^{1–108}$ with the following efficiencies: ClpAP ~ ClpXP > Lon >> FtsH under standard in vitro conditions (Fig. 4). However, whereas ClpXP degrades $RseA^{1–108}$ in the $RseA^{1–108}/\sigma^E$ complex as efficiently as free $RseA^{1–108}$, ClpAP and Lon degrade complexed $RseA^{1–108}$ more slowly than free $RseA^{1–108}$ and FtsH hardly degrades complexed $RseA^{1–108}$ at all. These results are in accord with the lower unfoldase activity of Lon (A. Matouschek, pers. comm.) and FtsH (Herman et al. 2003). We conclude that four of the five ATP-dependent proteases degrade $RseA^{1–108}$ in vitro, and three are also capable of catalyzing the disassembly of the $RseA^{1–108}/\sigma^E$ complex relatively efficiently.

Multiple ATP-dependent proteases participate in $RseA^{1–108}$ degradation in vivo

To identify the ATP-dependent proteases active against $RseA^{1–108}$ in vivo, we determined whether singly deficient protease strains were defective in degradation of $RseA^{1–108}$. Only disruption of *clpX* or *clpP* decreased the rate of degradation of $RseA^{1–108}$ (Fig. 5A; data not shown), validating previous data that indicated ClpXP as the major protease degrading $RseA^{1–108}$ (Flynn et al. 2004). However, as $RseA^{1–108}$ was degraded very rapidly in the absence of ClpXP ($T_{1/2}$ ~ 1.6 min) (Fig. 5A), additional proteases must be active in $RseA^{1–108}$ degradation in vivo.

We tested strains lacking multiple ATP-dependent proteases to identify the additional proteases participating in $RseA^{1–108}$ degradation (Fig. 5A; data not shown). The rate of degradation of $RseA^{1–108}$ in a Δ*clpA*Δ*clpX* strain was the same as that in a Δ*clpX* strain, even though formation of both the ClpAP and ClpXP proteases are prevented in this strain (data not shown). This result is consistent with the similar stabilization of $RseA^{1–108}$ in a Δ*clpX* and a Δ*clpP* strain (Fig. 5A) and suggests that ClpAP does not play a major role in degrading $RseA^{1–108}$ in vivo even though ClpAP was almost as efficient as ClpXP in degrading $RseA^{1–108}$ in vitro. In contrast, a Δ*clpX*Δ*lon* strain showed a reproducibly slower rate of degradation of $RseA^{1–108}$ ($T_{1/2}$ = 2.2 min) than the Δ*clpX* strain, suggesting that Lon is second to ClpXP in degrading $RseA^{1–108}$. Although this could be an indirect effect, the fact that Lon degrades $RseA^{1–108}$ in vitro suggests that the slower rate of degradation is likely to result from eliminating Lon-mediated turnover of RseA. A Δ*clpP*Δ*clpX*Δ*lon* strain showed a further and larger decrease in degradation of $RseA^{1–108}$ ($T_{1/2}$ = 3.5 min). One interpretation of these results is that when Lon is missing, ClpAP degrades $RseA^{1–108}$; removal of ClpP would prevent this latter degradation. Degradation by ClpAP is consistent with its rapid degradation of $RseA^{1–108}$ in vitro. Interestingly, a Δ*clpP*Δ*clpX*Δ*lon*Δ*hslUV* strain further decreases degradation of $RseA^{1–108}$ ($T_{1/2}$ = 4.0 min) even though HslUV did not degrade $RseA^{1–108}$ in vitro (see below). A Δ*clpP*Δ*clpX*Δ*lon*Δ*hslUV*Δ*clpA* strain degrades $RseA^{1–108}$ somewhat more slowly ($T_{1/2}$ = 5.5 min) (Fig. 5A), possibly because ClpA unfoldase function is removed. With the assistance of cytoplasmic protein unfoldases, FtsH may carry out this residual degradation, a proposition we did not test because *ftsH* is essential. In summary, successive removal of each ATP-dependent protease decreased the rate of degradation of $RseA^{1–108}$ in small incremental steps. Some of these decreases could be an indirect reflection of increased protease load on the remaining proteases. However, the fact that four of the five ATP-dependent proteases degrade $RseA^{1–108}$ in vitro suggests that the effect is direct. Taken together, these data make the key point that $RseA^{1–108}$ has evolved to be a substrate for many proteolytic machines, and as a consequence, even when the cytoplasmic proteolytic machinery is significantly disabled, $RseA^{1–108}$ is still degraded very rapidly.

The role of ATP-independent proteases in RseA$^{1–108}$ degradation

Given the requirement for disassembly, we have thus far solely considered the role of ATP-dependent proteases in degradation of RseA$^{1–108}$. However, the crystal structure of RseA$^{1–100}$/σ^E indicates that only the first 66 amino acids of RseA interact with σ^E; the remainder is predicted to be unstructured and has been found to have a binding site for the ClpX adaptor protein, SspB (Campbell et al. 2003; Flynn et al. 2004; Levchenko et al. 2005). This large unstructured tail might be a substrate for cleavage by ATP-independent proteases. The preferred cleavage site for RseP follows Ala 108; however, RseP might cleave other portions within the unstructured region at lower efficiency. We therefore tested whether removal of RseP, in addition to some ATP-dependent proteases, altered degradation of RseA$^{1–108}$ (Fig. 5B). Indeed, a Δ*clpX*Δ*rseP* strain degraded RseA$^{1–108}$ more slowly than a Δ*clpX* strain ($T_{1/2}$ = 2.0 min vs. $T_{1/2}$ = 1.6 min); likewise a Δ*clpX*Δ*lon*Δ*rseP* strain exhibited more stabilization of RseA$^{1–108}$ than the isogenic strain with intact *rseP* ($T_{1/2}$ = 3.5 min vs. $T_{1/2}$ = 2.2 min). Cleavage by RseP in the unstructured tail might generate a new cytoplasmic variant of RseA that is a substrate for additional proteases, such as HslUV, thereby rationalizing degradation of RseA$^{1–108}$ by HslUV in vivo, but not in vitro.

The activity of σ^E is relatively insensitive to the flux of substrates through ClpXP

The substrate load for the cytoplasmic proteases undoubtedly varies with growth conditions. We asked whether σ^E activity was sensitive to substrate load on ClpXP, the major protease degrading RseA$^{1–108}$. Major substrates of ClpXP are σ^S and ssrA-tagged proteins (Schweder et al. 1996; Gottesman et al. 1998). We tested whether decreasing the flux of these substrate proteins through ClpXP increases the rate of degradation of RseA$^{1–108}$. As endogenous RseA$^{1–108}$ is not observable on Western blots in wild-type cells due to its rapid degradation, we overproduced RseA$^{1–108}$ and compared its accumulation in wild-type and mutant strains. Both a Δ*ssrA* strain (which lacks ssrA-tagged substrates) and a Δ*rssB* strain (which lacks the protein that targets σ^S to ClpX) accumulated less RseA$^{1–108}$ than the wild-type strain (Fig. 6A), indicating that degradation of RseA$^{1–108}$ increased when competing substrates are eliminated.

We next asked whether increased degradation of RseA$^{1–108}$ observed in Δ*ssrA* and Δ*rssB* strains resulted in altered σ^E activity. Note that in these experiments, strains do not contain the RseA$^{1–108}$ overexpression construct: All forms of RseA are generated exclusively by the endogenous protease cascade. We find that with or without induction of the YYF peptide, Δ*ssrA* (Fig. 6B, top) and Δ*rssB* (Fig. 6B, bottom) have σ^E activity equivalent to that of the wild-type strain even though RseA$^{1–108}$ was degraded more rapidly in the mutant strain backgrounds (Fig. 6A). This result is in agreement with our finding that the initial cleavage step is the slowest in the pathway and shows that this kinetic arrangement makes σ^E activity insensitive to perturbations that result in increased degradation of RseA$^{1–108}$.

The activity of σ^E is relatively insensitive to fluctuations in the level of ClpX

As ClpXP is the major cytoplasmic protease that degrades RseA$^{1–108}$ to liberate σ^E, we tested the effect of removing ClpX on σ^E activity, which stabilizes RseA$^{1–108}$ approximately fivefold ($T_{1/2}$ = 1.6 min in a Δ*clpX* strain vs. 20 sec in wild type) (Fig. 5A). Under noninducing conditions, the σ^E activity of a Δ*clpX* strain was comparable to that of the wild-type (Fig. 6C), indicating that the increased stability of RseA$^{1–108}$ does not affect transcriptional activity. This is expected, because initial cleavage by DegS is much slower than the rate of final degradation of RseA$^{1–108}$ under noninducing conditions. Under inducing conditions, the σ^E activity of a Δ*clpX* strain is

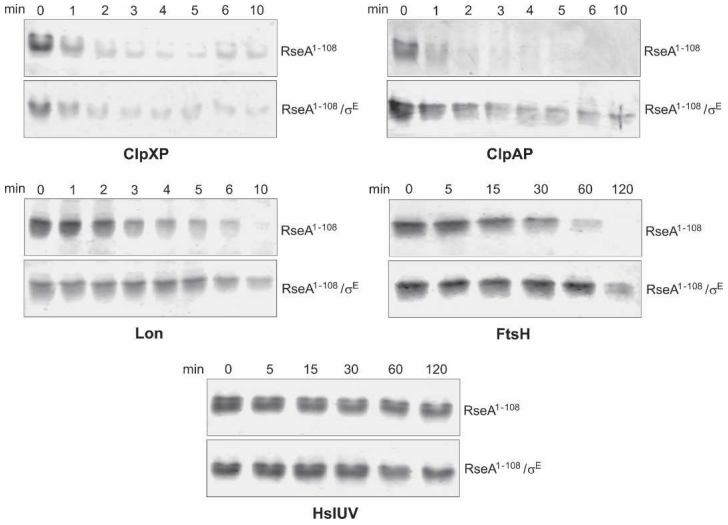

Figure 4. Multiple ATP-dependent proteases degrade RseA$^{1–108}$ in vitro. Degradation of RseA$^{1–108}$ alone or RseA$^{1–108}$ in complex with σ^E (RseA$^{1–108}$/σ^E) by ATP-dependent proteases was carried out as described in Materials and Methods. Samples were removed at the defined time intervals, separated by SDS-PAGE, and stained with Sypro Ruby protein gel stain. Bands were visualized by a FluorImager.

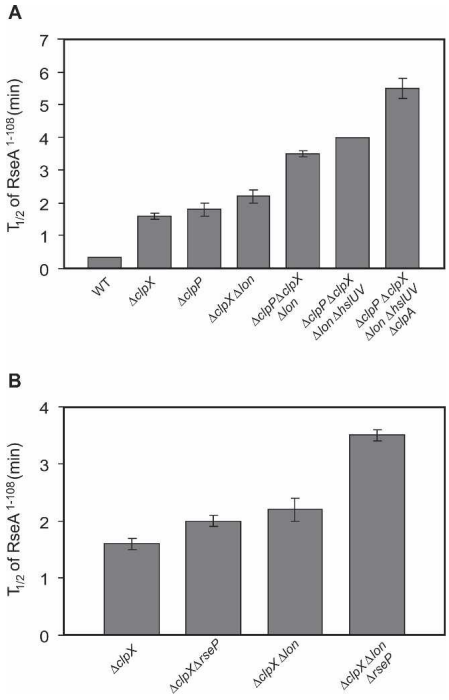

Figure 5. Multiple proteases degrade RseA$^{1–108}$ in vivo. (*A*) Multiple ATP-dependent proteases degrade RseA$^{1–108}$ in vivo. The stability of RseA$^{1–108}$ was measured upon overexpression of RseA$^{1–108}$/σ^E in wild-type (WT, CAG53209), Δ*clpX* (CAG53193), Δ*clpP* (CAG53194), Δ*clpX*Δ*lon* (CAG53195), Δ*clpP*Δ*clpX*Δ*lon* (CAG53217), Δ*clpP*Δ*clpX*Δ*lon*Δ*hslUV* (CAG53220), and Δ*clpP*Δ*clpX*Δ*lon*Δ*hslUV*Δ*clpA* (CAG53228) as described in the legend for Figure 2C. Data shown are the average of at least two independent experiments. (*B*) RseP is involved in degrading RseA$^{1–108}$ in vivo. The stability of RseA$^{1–108}$ was measured upon overexpression of RseA$^{1–108}$/σ^E in Δ*clpX*Δ*rseP* (CAG53206) and Δ*clpX*Δ*lon*Δ*rseP* (CAG53215), and their isogenic strains with intact *rseP* (CAG53193 and CAG53195) as described in the legend for Figure 2C. Note that the σ^E supplied on the plasmid allows us to delete *rseP*, which is essential in wild-type strains. Data shown are the average of at least two independent experiments.

induced ~1.5-fold to twofold less than that of the wild-type strain (Fig. 6C; Flynn et al. 2004). Two factors contribute to lower activity in the Δ*clpX* strain. First, initial DegS cleavage is slower than in the wild-type strain (Fig. 6C, inset: $T_{1/2}$ = 1.1 min for wild type vs. 1.9 min for Δ*clpX*), possibly because physiological changes in Δ*clpX* cells might indirectly alter membrane proteolysis. Second, degradation of RseA$^{1–108}$ in Δ*clpX* cells ($T_{1/2}$ = 1.6 min) is now comparable to the rate of RseA cleavage by DegS ($T_{1/2}$ = 1.9 min), so that DegS cleavage and degradation by cytoplasmic proteases become colimiting. The net result is a somewhat slower generation of free σ^E. We note that the magnitude of the defect in σ^E induction is significantly less than the magnitude of the proteolytic defect. Thus, the organization of the proteolytic cascade decreases the sensitivity of σ^E activity to alterations in the proteolytic environment of the cell that diminish degradation of RseA$^{1–108}$.

Discussion

The goal of this study was to investigate the design principles that permit a protease cascade to convert a signal generated in the envelope to an immediate change in the activity of a transcription factor. To this end, we examined individual steps in the proteolytic pathway that

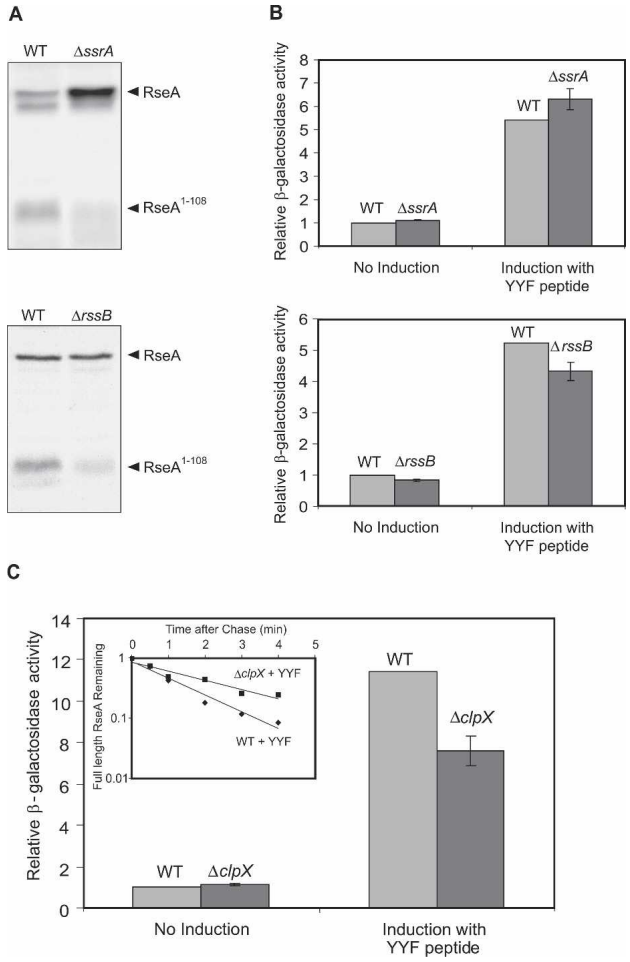

Figure 6. σ^E activity is relatively insensitive to the flux of substrates through ClpXP (*A*,*B*) and fluctuations in the level of ClpX (*C*). (*A*) In order to compare the rate of degradation of RseA$^{1–108}$ in wild-type and mutants, RseA$^{1–108}$ was overexpressed in Δ*ssrA* (CAG53162) and Δ*rssB* (CAG53144), and their isogenic wild-type strains (CAG53153 and CAG53092). Samples were separated by SDS-PAGE and probed with antibodies against the cytoplasmic domain of RseA. (*B*) Relative σ^E activity of wild-type (WT, CAG43450), Δ*ssrA* (CAG53073), and Δ*rssB* (CAG53072) strains. Cells were grown in LB at 30°C to O.D.$_{600}$ of 0.1–0.15 and expression of YYF peptide was induced with IPTG. β-Galactosidase activities were measured as described in Materials and Methods. Data shown are the average of three independent experiments. (*C*) Relative σ^E activity of wild-type (WT, CAG53077) and Δ*clpX* (CAG53078) strains was determined as described for *B*. (*Inset*) The rate of cleavage of full-length RseA by DegS in wild-type (WT, CAG53077) and Δ*clpX* (CAG53078) strains upon induction of YYF peptide was determined by measuring the stability of RseA as described in Materials and Methods. A representative data set is shown.

controls the activity of the essential transcription factor σ^E by regulating the degradation of the anti-σ factor, RseA. Our major findings are that the signal-sensing cleavage step initiating the pathway is rate-limiting under all conditions, that this proteolysis pathway is robust to changes in the activity of cytoplasmic proteases, and that free σ^E is released almost exclusively by proteolysis. Below we discuss the construction principles that underlie each of these characteristics and their biological significance.

Organization of the proteolytic cascade

The proteolytic cascade consists of three sequential steps: a ligand-activated, initial cleavage step carried out by DegS, in which RseA is cleaved in the periplasmic domain; a highly regulated (possibly conformationally controlled) second step carried out by the RIP protease, RseP, which releases the $RseA^{1–108}/\sigma^E$ complex from the membrane; and a final disassembly-degradation step, carried out by multiple ATP-dependent proteases within the cytoplasmic compartment of the cell (Figs. 1, 4, 5A; Ades et al. 1999; Alba et al. 2002; Kanehara et al. 2002; Walsh et al. 2003; Akiyama et al. 2004; Flynn et al. 2004). This last step releases free σ^E, which binds to RNA polymerase and promotes transcription of the σ^E-regulon to combat envelope stress.

This work demonstrates that even under inducing conditions, the signal-sensitive DegS cleavage step is the slowest in the proteolytic cascade ($T_{1/2}$ = 1 min); the two subsequent steps are each at least threefold faster than the initiating cleavage step (Fig. 2). This arrangement ensures that the overall rate of degradation of the protein reflects the status of the signal up to DegS cleavage rates as rapid as $T_{1/2} \sim 30$ sec.

DegS-independent cleavage of RseA by RseP (a RIP protease) is highly controlled; whereas full-length RseA is cleaved very slowly by RseP, DegS-processed RseA is cleaved rapidly (Alba et al. 2002; Kanehara et al. 2002). The mechanistic details underlying this are unknown; however DegS, RseB, the periplasmic domain of RseA, and the PDZ domain of RseP participate in at least two independent mechanisms to repress activity of this protease toward full-length RseA (Kanehara et al. 2003; Bohn et al. 2004; Grigorova et al. 2004). We have suggested that RseP cleavage of full-length RseA is blocked so that DegS cleavage of RseA will be rate-limiting over a wide range of OMP signal. Interestingly, other RIP proteases that are widely used to transmit signals via a protease cascade between the compartments of a bacterial cell appear to occupy an intermediate position in every cascade: They transmit the signal rather than initiate the cascade and their activity is inhibited until the initial cleavage event is completed (Schobel et al. 2004; Chen et al. 2005; Matson and DiRita 2005). Cells use widely different proteins to accomplish inhibition; it remains an open question as to whether these inhibitory events are mechanistically similar or distinct (Resnekov and Losick 1998; Dong and Cutting 2003; Zhou and Kroos 2004, 2005). It will be interesting to examine how quantitative relationships between initial and RIP-mediated cleavages further the output goals of several different systems.

Free σ^E is released only after degradation of $RseA^{1–108}$. This point in the pathway could provide an opportunity for a second regulatory step: $RseA^{1–108}$ might be treated as a dead-end product to be eliminated at all costs; alternatively, its degradation (and σ^E activity) might be modulated in concert with other proteolytic events keyed to the stress status of the cell; for example, the rate of degradation of σ^S. To examine this issue, we performed a careful analysis of the proteases degrading $RseA^{1–108}$ and investigated the cellular consequences of increasing or decreasing the rate of degradation of $RseA^{1–108}$. These studies together with other data provide a clear answer: The cell uses multiple mechanisms to ensure that $RseA^{1–108}$ is degraded regardless of the proteolytic status of the cell. First, $RseA^{1–108}$ is the most rapidly degraded substrate of its major protease, ClpXP ($T_{1/2} \leq 20$ sec) (Fig. 2C). Thus, DegS cleavage will remain rate-limiting even if competing substrates slightly decrease its rate of degradation by ClpXP. Second, in the unlikely event that ClpXP is overwhelmed by other substrates, $RseA^{1–108}$ is degraded rapidly by other proteases ($T_{1/2}$ = 1.6 min), leaving DegS cleavage of RseA rate-limiting under a broad range of conditions and thereby ensuring minimal effects on σ^E activity (Fig. 6C). Finally, the two major proteases that degrade $RseA^{1–108}$, ClpXP and Lon, are both in the σ^E-regulon (Rhodius et al. 2006). Hence, under conditions inducing σ^E, the amount of these proteases will increase to further ensure that DegS cleavage remains rate-limiting. It will be interesting to determine whether uncoupling of degradation rate from the proteolytic status of cytoplasmic proteases is a general characteristic of systems regulated by unstable anti-σs.

$RseA^{1–108}$ is the first protein identified to be a substrate of all of the ATP-dependent proteases. This allowed us to examine the interconnections between these proteases. Our most important finding was that ClpAP degrades $RseA^{1–108}$ very poorly in vivo even though it degrades both free and σ^E-bound $RseA^{1–108}$ almost as well as ClpXP in vitro. The low activity of ClpAP in vivo cannot be explained by ClpS or SspB inhibition of ClpAP (Flynn et al. 2001; Dougan et al. 2002; Farrell et al. 2005) as ClpAP still has very little activity against $RseA^{1–108}$ in Δ*clpS*, Δ*sspB* and Δ*clpS*Δ*sspB* strains (R. Chaba, unpubl.; data not shown). Possibly, a currently unidentified inhibitor may prevent ClpAP from degrading $RseA^{1–108}$ in vivo. Additionally, our data raises the possibility that HslUV degrades $RseA^{1–108}$ in vivo, but not in vitro. The simplest explanation for this discrepancy is that ATP-independent protease(s) expose an HslUV-degradation tag; more complex explanations, such as an unidentified HslUV-adaptor protein needed for substrate recognition, can be envisioned. Our study suggests that RseP might be a candidate protease to expose an HslUV recognition signal. Previous studies indicated that RseP cleaves RseA only at a single position, both in vivo and in vitro, which resulted in generation of $RseA^{1–108}$. However, these studies were performed on an artificial substrate, with

both cytoplasmic and periplasmic domains replaced by entities more amenable to analysis (Akiyama et al. 2004). $RseA^{1–108}$ has a long extended tail; it is possible that RseP cleaves at additional positions within this tail or at other unstructured regions of the protein under conditions where degradation of $RseA^{1–108}$ is delayed (Campbell et al. 2003). We plan to test this idea as it would be the first indication that a RIP protease can act on the cytoplasmic portion of a protein.

Transducing the degradation signal to a change in activity of σ^E

σ^E and $RseA^{1–100}$ bind extremely tightly; their picomolar affinity is comparable to that of an antigen–antibody interaction. This exceptionally tight binding is explained by the extensive interface between the two proteins: $RseA^{1–100}$ is sandwiched between the two domains of σ^E, making extensive interactions with each domain, and burying a total surface area of 3805 Å^2 (Campbell et al. 2003). To dissociate spontaneously, σ^E would need to break all of these interactions, a situation that rarely occurs. Instead, σ^E is released by an extremely efficient disassembly-degradation reaction catalyzed by the cytoplasmic ATP-dependent proteases, which occurs with a $T_{1/2}$ of <20 sec.

Why does the cell use the energy intensive process of disassembly and degradation of $RseA^{1–108}$ to set the rate of σ^E release directly rather than relying solely on indirectly regulating free σ^E by changing the relative levels of RseA and σ^E? This latter scenario avoids the high-energy cost of dissociating the two proteins because it does not require very tight binding between σ^E and RseA. Modeling kinetics of down-regulation of σ^E activity in each scenario, as demonstrated in Figure 7, provides a possible answer. σ^E down-regulation results from a decrease in the DegS activating signal, which translates into decreased DegS cleavage of RseA, such as occurs after temperature downshift (Ades et al. 2003). In a dissociation-dependent scenario, free σ^E (and thus σ^E activity) is set by the relative levels of RseA and σ^E. RseA levels rise slowly in response to its decreased degradation (Fig. 7A, top); free σ^E drops in concert with the rise in RseA level (Fig. 7A, bottom), resulting in a slow decrease in σ^E activity. In contrast, when free σ^E is generated solely by proteolysis, RseA stabilization results in a rapid decrease in free σ^E (Fig. 7B, bottom) prior to any change in the relative levels of RseA and σ^E (Fig. 7B, top) provided that RseA is at least stoichiometric with σ^E. Intuitively, the rapid drop in free σ^E is explained by the fact that the rate of σ^E release would slow immediately upon a decrease in RseA degradation, while any preexisting σ^E rapidly reassociates with RseA (Fig. 3C). Published data and our unpublished results suggest that RseA is in excess over σ^E under basal conditions (Ades et al. 2003) and the high rate of synthesis of RseA relative to σ^E under inducing conditions (Ades et al. 2003) suggests that this scenario is possible under inducing conditions as well. Results from this scenario fit well with experimental determinations, indicating that σ^E exhibits a 10-fold decrease in activity within a few minutes after temperature downshift, at a time when the RseA::σ^E ratio is virtually unchanged from its value at high temperature (Ades et al. 2003). This situation obtains because RseA stabilization is compensated by decreased synthesis from its σ^E-dependent promoter. Likewise, in accordance with the proteolysis-controlled model, upon temperature upshift, increase in σ^E activity occurs prior to change in the RseA::σ^E ratio (I. Grigorova, unpubl.; data not shown). Only extreme inducing signals, such as continuous overexpression of outer membrane porins, lead to a significant change in the RseA::σ^E ratio, possibly because degradation overwhelms synthesis (Ades et al. 1999). In conclusion, physiological inducing signals that trigger DegS-mediated cleavage of RseA, work by increasing the dynamics of RseA production and degradation and therefore the dynamics of binding and release of σ^E, rather than by rapidly changing the level of RseA.

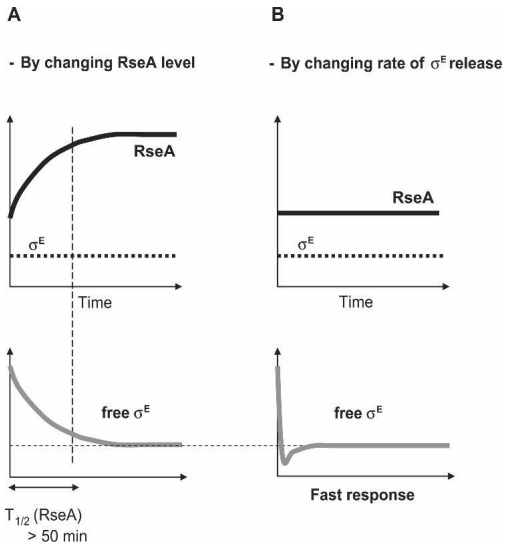

Figure 7. Two scenarios by which stabilization of RseA could decrease σ^E activity. (*A*) An increase in the level of RseA relative to that of σ^E decreases σ^E activity. (*Top*) Analytical calculation of the change in RseA level resulting from changing its rapid degradation at 43°C ($T_{1/2}$ = 2 min) to its slow degradation at 30°C ($T_{1/2}$ > 50 min) (Ades et al. 2003), reveals that the characteristic time of RseA increase upon temperature downshift is on the order of tens of minutes. (*Bottom*) Thus, a decrease in the level of free σ^E (σ^E not bound to RseA), which determines σ^E activity, occurs very slowly in concert with the rise in RseA. (*B*) A decrease in the rate of σ^E release from RseA decreases σ^E activity. This scenario requires that the degradation rate of RseA >> the dissociation rate of RseA from σ^E. Computer simulation of a quantitative model of our system using parameters determined experimentally in this work and Ades et al. (2003) (RseA degradation, σ^E and RseA synthesis, dilution by cell growth, and binding) (data not shown) demonstrated that decreased release of σ^E into the cytoplasm as a consequence of decreased initiation of RseA degradation by DegS would result in rapid down-regulation of free σ^E (*bottom*) on a time scale much faster than changes in the relative levels of the two proteins (*top*). This scenario does not require changes in the relative levels of σ^E and RseA.

The tight coupling of proteolysis and activity found in the RseA/σ^E pathway might be important for other Group 4 (ECF) σs in addition to σ^E. Group 4 σs comprise the majority of the alternate σs, and they control a wide range of responses to environmental stress in diverse bacteria. A predominant paradigm is these ECF σs positively control their own transcription and are located in operons together with their anti-σ regulators (Missiakas and Raina 1998; Raivio and Silhavy 2001; Bashyam and Hasnain 2004). These anti-σs are often regulated by proteolysis and show increased degradation when stress increases and decreased degradation when stress decreases (Browning et al. 2003; Schobel et al. 2004; Reiling et al. 2005). We suspect that the ability to immediately downregulate activity in response to decreased proteolysis will be an important design principle for the proteolytic cascades governing the activity of many Group 4 σs and possibly in other systems governed by unstable negative regulators.

Materials and methods

Media, antibiotics, strains, and plasmids

Luria-Bertani (LB) and M9 minimal medium were prepared as described (Sambrook et al. 1989). M9 was supplemented with 0.2% glucose, 1 mM $MgSO_4$, 2 μg/mL thiamine, and all amino acids (40 μg/mL), except methionine. When required, the medium was supplemented with 100 μg/mL ampicillin (Ap), 20 μg/mL chloramphenicol (Cm), 30 μg/mL kanamycin (Kan), 50 μg/mL spectinomycin (Spec), and/or 10 μg/mL tetracycline (Tet). Expression of proteins from T7, Ptrc, or mutated Ptrc promoters was induced by 1 mM isopropyl-β-D-thiogalactopyranoside (IPTG).

Table 1. *Strains and plasmids used in this study*

Strains/plasmids	Relevant genotype	Source/reference
Strains		
BL21(DE3)	F$^-$ *ompT gal dcm lon hsdS*$_B$(r$_B^-$ m$_B^-$) λ(DE3)	Studier and Moffatt 1986
MC1061	*araD* Δ*(ara-leu)7697* Δ*(codB-lacI) galK16 galE15 mcrA0 relA1 rpsL150 spoT1 mcrB9999 hsdR2*	Casadaban and Cohen 1980; *E. coli* Genetic Stock Center
MG1655	*rph*-1	Guyer et al. 1981; Jensen 1993; *E. coli* Genetic Stock Center
CAG16037	MC1061 [ϕλ*rpoH* P3::*lacZ*]	Mecsas et al. 1993
CAG45114	MG1655 [ϕλ*rpoH* P3::*lacZ*]	Ades et al. 2003
CAG43450	16037 pBA166, Ap^R	Walsh et al. 2003
CAG53072	43450 *rssB*::*kanR*, Kan^R Ap^R	This work
CAG53073	43450 *ssrA*::*kanR*, Kan^R Ap^R	This work
CAG53077	45114 pBA166, Ap^R	This work
CAG53078	53077 *clpX*::*kanR*, Kan^R Ap^R	This work
CAG53092	45114 pRC8, Ap^R	This work
CAG53144	53092 *rssB*::*kanR*, Kan^R Ap^R	This work
CAG53153	16037 pRC8, Ap^R	This work
CAG53162	53153 *ssrA*::*kanR*, Kan^R Ap^R	This work
CAG53193	45114 *clpX*::*kanR* pRC14, Kan^R Ap^R	This work
CAG53194	45114 *clpP*::*cmR* pRC14, Cm^R Ap^R	This work
CAG53195	53193 *lon*::*tetR*, Kan^R Tet^R Ap^R	This work
CAG53206	53193 *rseP*::*specR*, Kan^R Spec^R Ap^R	This work
CAG53209	45114 pRC14, Ap^R	This work
CAG53215	53195 *rseP*::*specR*, Kan^R Tet^R Spec^R Ap^R	This work
CAG53217	45114 *clpPclpXlon*::*cmR* pRC14, Cm^R Ap^R	This work
CAG53218	53217 *clpA*::*kanR*, Cm^R Kan^R Ap^R	This work
CAG53220	53217 *hslUV*::*tetR*, Cm^R Tet^R Ap^R	This work
CAG53228	53218 *hslUV*::*tetR*, Cm^R Kan^R Tet^R Ap^R	This work
Plasmids		
pBA166	YYF peptide in pTrc99a, Ap^R	Walsh et al. 2003
pJT6	his$_6$-RseA$^{1–100}$ in pET28b, Kan^R	This work
pPER76	his$_6$-σ^E in pET15b, Ap^R	Rouviere et al. 1995
pRC8	RseA$^{1–108}$ in pBA169, Ap^R	This work
pRC10	–10 box of Ptrc changed to Plac in pBA169, Ap^R	This work
pRC14	RseA$^{1–108}$ and σ^E in pRC10, Ap^R	This work
pRseA$^{1–100}$E28C	his$_6$-RseA$^{1–100}$E28C in pET28b, Kan^R	This work
pET15b	Vector, pBR322 ori, Ap^R	Novagen
pET28b	Vector, pBR322 ori, Kan^R	Novagen
pTrc99a	Vector, pBR322 ori, Ap^R	Amersham Pharmacia Biotech
pBA169	pTrc99a Δ*Nco*I, Ap^R	Walsh et al. 2003

Strains and plasmids are listed in Table 1. Most experiments used MG1655; comparable results were obtained with MC1061. Details of plasmid construction are available on request.

Buffers

Buffer I comprises 10 mM Tris-HCl (pH 9.0), 5% glycerol, 0.1 mM aminoethylbenzenesulfonic acid (AEBSF), and 0.5 mM β-mercaptoethanol (BME).

PD buffer contains 25 mM HEPES-KOH (pH 7.5), 5 mM KCl, 5 mM $MgCl_2$, 0.02% NP-40, and 10% glycerol. HO buffer contains 50 mM HEPES-KOH (pH 7.5), 20 mM $MgCl_2$, 300 mM NaCl, 10% glycerol, and 0.5 mM DTT. Buffer H consists of 50 mM Tris-HCl (pH 7.6), 100 mM KCl, 25 µM zinc acetate, 0.1% NP-40, 10 mM $MgCl_2$, and 1 mM DTT. Lon buffer contains 50 mM Tris-HCl (pH 8.0), 5 mM KCl, 15 mM $MgCl_2$, and 2 mM DTT.

Proteins

ClpA (Maurizi et al. 1994), ClpP (Kim et al. 2000), ClpX (Levchenko et al. 1997), FtsH (Herman et al. 2003), HslU, HslV (Burton et al. 2005), Lon (Goldberg et al. 1994), $RseA^{1–108}$, and σ^E (Flynn et al. 2004) were purified as described.

For the purification of his_6-σ^E, his_6-$RseA^{1–100}$, and his_6-$RseA^{1–100}$E28C, plasmids pPER76, pJT6, and p$RseA^{1–100}$E28C were transformed in BL21(DE3). Cultures were grown at 37°C in LB containing appropriate antibiotics to an $O.D._{600}$ ~ 0.5 and induced with IPTG for 1–2 h; harvested cells were subjected to three freeze/thaw cycles in liquid nitrogen and ice water. Cells were resuspended in Buffer I/500 mM NaCl/10 mM imidazole (pH 7.9) containing 200 µg/mL lysozyme and lysed by sonication. After centrifugation, the supernatant was applied to Co^{2+} metal ion affinity column (Talon resin, Clontech) equilibrated in Buffer I/500 mM NaCl/10 mM imidazole. The column was washed with Buffer I/500 mM NaCl/20 mM imidazole and step-eluted with Buffer I/150 mM NaCl/40, 60, 100, 200 mM imidazole. The eluted protein was dialyzed against Buffer I/50 mM NaCl/25% glycerol/0.1% Tween 20. The Co^{2+} elution pool was further loaded on HiTrap Q (Pharmacia) anion exchange column equilibrated in Buffer I/50 mM NaCl. The Q column was washed with equilibration buffer and step-eluted with Buffer I/100, 250 mM NaCl. Fractions containing protein were pooled, dialyzed against the dialysis buffer, flash-frozen in liquid nitrogen, and stored at –80°C.

Fluorescent labeling

Prior to fluorescent labeling with rhodamine on cysteine 28, his_6-$RseA^{1–100}$E28C purified on HiTrap Q anion exchange column was loaded on PD10 desalting column. The protein was eluted using dialysis buffer without BME. The protein was incubated with 10-fold molar excess of rhodamine maleimide (Molecular Probes) at 4°C for 2 h The reaction was quenched with 1000-fold excess of DTT and the sample was centrifuged at 4°C to remove precipitated dye. In order to remove unreacted dye, the supernatant was chromatographed on PD10 desalting column prewashed with dialysis buffer containing 2 mM DTT. Fractions were analyzed by Coomassie staining of SDS-PAGE gels and by fluorescent imaging using Alpha Imager 2000.

Polarization anisotropy

His_6-$RseA^{1–100}$E28C freshly labeled with rhodamine, unlabeled his_6-σ^E, and his_6-$RseA^{1–100}$ were diluted to appropriate concentration using dialysis buffer without glycerol. The samples were degassed under vacuum at room temperature before data collection. Data was collected with a K2 Multifrequency Fluorimeter (ISS) set to λ_{ex} = 543 nm and λ_{em} = 575 nm.

The binding curve of labeled his_6-$RseA^{1–100}$E28C and his_6-σ^E was obtained by measuring polarization anisotropy for 100 nM labeled his_6-$RseA^{1–100}$E28C in the presence of various concentrations of his_6-σ^E. Relative affinities of labeled his_6-$RseA^{1–100}$E28C and unlabeled his_6-$RseA^{1–100}$ were measured by adding different concentrations of his_6-σ^E to the mixture of labeled and unlabeled proteins (100 nM each protein). Both the proteins bound his_6-σ^E with the same affinity. The dissociation rate of labeled his_6-$RseA^{1–100}$E28C/his_6-σ^E complex (100 nM) was measured by monitoring anisotropy of the complex upon addition of excess unlabeled his_6-$RseA^{1–100}$ (1.5 µM). The dissociation rate of unlabeled his_6-$RseA^{1–100}$/his_6-σ^E complex was measured in a similar manner in the presence of excess labeled his_6-$RseA^{1–100}$E28C.

Kinetic assay

The time course of his_6-σ^E binding to labeled his_6-$RseA^{1–100}$E28C was obtained by following the increase in rhodamine fluorescence intensity (λ_{ex} = 543 nm, λ_{em} = 575 nm) upon formation of the complex, using a stopped flow hand-operated mixing system (SFA-20; HiTech Scientific) and fluorimeter (K2; ISS). To calculate the association rate constant of his_6-σ^E and labeled his_6-$RseA^{1–100}$E28C, the time course of their binding was measured for various concentrations of the two proteins (125 nM and 128 nM; 247 nM and 128 nM; 250 nM and 100 nM; 128 nM and 370 nM of his_6-σ^E and labeled his_6-$RseA^{1–100}$E28C). The data was analyzed using Kaleidagraph (Synergy Software) by fitting to the function shown in Equation 1.

$$I = I_0 + \Delta I \cdot C, \text{ where}$$

$$C = \frac{\sigma^E \cdot \exp\{-k \cdot |(\sigma^E - RseA_{cyto})| \cdot t\} - 1}{RseA_{cyto} \cdot \exp\{-k \cdot |(\sigma^E - RseA_{cyto})| \cdot t\} - \sigma^E} \quad \text{(Eq. 1)}$$

where I_0 is the fluorescence intensity of labeled his_6-$RseA^{1–100}$ E28C not in complex with his_6-σ^E, ΔI is the increase in fluorescence intensity upon his_6-σ^E binding, C is the fraction of labeled his_6-$RseA^{1–100}$ E28C in complex with his_6-σ^E, σ^E and $RseA_{cyto}$ are the concentrations of his_6-σ^E and labeled his_6-$RseA^{1–100}$ E28C mixed together, and k is the association rate constant.

Determination of RseA, RseA-I, and $RseA^{1–108}$ stability by pulse-chase immunoprecipitation

Cells were grown in supplemented M9 minimal medium lacking methionine (with 100 µg/mL Ap) at 30°C to an $O.D._{450}$ of 0.15–0.25. Cultures were induced with IPTG for 10 min to overexpress YYF peptide or $RseA^{1–108}$/σ^E. Cells were pulse-labeled for 15 sec with L-[^{35}S] methionine followed by a chase of 0.1% unlabeled methionine. Samples were processed as described (Ades et al. 2003). As an internal standard, an equal amount of extract from L-[^{35}S] methionine-labeled cells overexpressing the truncated form of RseA, HA-RseA140 (also designated as RseA* in the text) (Kanehara et al. 2002) was added to each sample prior to immunoprecipitation. Samples were immunoprecipitated with antibodies against the cytoplasmic domain of RseA. $T_{1/2}$ of RseA and $RseA^{1–108}$ was determined as described (Ades et al. 2003). To estimate the $T_{1/2}$ of RseA-I, both accumulation and disappearance of this intermediate on the gel was quantified. The net generation of RseA-I resulting from RseA cleavage by DegS and its disappearance upon cleavage by RseP can be described by Equation 2, where k_{DegS} and k_{RseP} are the rate con-

stants of RseA cleavage by DegS and RseA-I cleavage by RseP, respectively.

$$RseA - I \sim \frac{k_{DegS}}{k_{RseP} - k_{DegS}} \cdot \{\exp(-k_{DegS}t) - \exp(-k_{RseP}t)\} \quad \text{(Eq. 2)}$$

Maximal accumulation of RseA-I was measured to be between 25 and 50 sec after the chase. Using the value for k_{DegS} determined as described (Ades et al. 2003) and Equation 3, we have estimated k_{RseP} and thus the $T_{1/2}$ of RseA-I.

$$(k_{RseP} - k_{DegS}) \cdot t_{\max} = \ln\left(\frac{k_{RseP}}{k_{DegS}}\right) \quad \text{(Eq. 3)}$$

$T_{1/2}$ of RseA-I can be also estimated from the ratio of RseA-I to RseA that does not change with time at longer time points. For this, we quantified the ratio of RseA-I to RseA at each time point and calculated $T_{1/2}$ of RseA-I using Equation 4.

$$\frac{RseA - I}{RseA} = \frac{k_{DegS}}{k_{RseP} - k_{DegS}} \cdot \{1 - \exp(k_{DegS} - k_{RseP}) \cdot t\} \quad \text{(Eq. 4)}$$

The $T_{1/2}$ of RseA-I measured using Equation 4 was in good agreement with that measured using Equations 2 and 3.

Degradation assays

In order to monitor the degradation of $RseA^{1-108}$, ATP-dependent proteases ($ClpX_6$: 0.3 μM and $ClpP_{14}$: 0.8 μM for ClpXP; $ClpA_6$: 0.3 μM and $ClpP_{14}$: 0.8 μM for ClpAP; $HslU_6$: 0.3 μM and $HslV_{12}$: 0.8 μM for HslUV; Lon_6: 0.3 μM; $FtsH_6$: 0.3 μM), ATP (4 mM) and an ATP regeneration system (50 μg/mL creatine kinase and 2.5 mM creatine phosphate) were mixed in the appropriate buffer and incubated for 2 min at either 30°C or 37°C. $RseA^{1-108}$ (2 μM) or $RseA^{1-108}/\sigma^E$ (the complex was formed by incubating 2 μM of $RseA^{1-108}$ with 4 μM σ^E at 30°C for 10 min) was added to initiate the reaction. Samples were removed at various intervals, electrophoresed on SDS-PAGE, and visualized using Sypro Ruby protein gel stain (Molecular Probes) on a FluorImager 595 (Molecular Dynamics).

Degradation assays with ClpAP and ClpXP were performed at 30°C, whereas for FtsH, HslUV, and Lon the reactions were carried out at 37°C. Buffer condition was HO buffer for ClpAP, PD buffer for ClpXP and HslUV, Buffer H for FtsH, and Lon buffer for Lon.

Western blotting

The level of $RseA^{1-108}$ and σ^E was monitored by Western blot analysis. Cultures were grown in LB (with 100 μg/mL Ap) at 30°C to an $O.D._{600} \sim 0.3$ and induced with IPTG for 1 h. Samples were processed as described (Alba et al. 2001) and transferred to PVDF membrane. The following dilutions of primary antisera (all rabbit) were used: anti-RseA cytoplasmic domain (1:5000) and anti-σ^E (1:10,000). The secondary antibody (used at 1:10,000) was an anti-rabbit HRP (Amersham Life Sciences). Blots were developed with SuperSignal West Dura Extended Duration Substrate (Pierce). Epi Chemi II Darkroom (UVP Laboratory Products) was used to capture the light emitted from the blots. The intensity of the bands was quantified using associated software (Labworks).

β-Galactosidase assays

Overnight cultures were diluted to an $O.D._{600} \sim 0.015$ in LB with 100 μg/mL Ap and grown at 30°C to an $O.D._{600}$ of 0.1–0.15. Cultures were induced with IPTG to overexpress YYF peptide. σ^E activity was measured by monitoring β-galactosidase expression from a single-copy σ^E-dependent *lacZ* reporter gene as described (Miller 1972; Mecsas et al. 1993; Ades et al. 1999). All assays were performed three times to ensure reproducibility of the data.

Acknowledgments

We thank Mark Dayle and Dyche Mullins for help with the fluorescent anisotropy experiments and Jennifer Hou for help with SspB and ClpS/ClpAP experiments. We also thank members of the Gross laboratory for critically reading the manuscript. This work was supported by National Institutes of Health (NIH) Grants GM-32678 (to C.A.G) and GM-049224 (to T.A.B). I.L.G was supported by Burroughs Wellcome Predoctoral Fellowship. T.A.B and J.M.F are employees of HHMI.

References

Ades, S.E., Connolly, L.E., Alba, B.M., and Gross, C.A. 1999. The *Escherichia coli* σ^E-dependent extracytoplasmic stress response is controlled by the regulated proteolysis of an anti-σ factor. *Genes & Dev.* **13:** 2449–2461.

Ades, S.E., Grigorova, I.L., and Gross, C.A. 2003. Regulation of the alternative σ factor σ^E during initiation, adaptation, and shutoff of the extracytoplasmic heat shock response in *Escherichia coli*. *J. Bacteriol.* **185:** 2512–2519.

Akiyama, Y., Kanehara, K., and Ito, K. 2004. RseP (YaeL), an *Escherichia coli* RIP protease, cleaves transmembrane sequences. *EMBO J.* **23:** 4434–4442.

Alba, B.M., Zhong, H.J., Pelayo, J.C., and Gross, C.A. 2001. degS (hhoB) is an essential *Escherichia coli* gene whose indispensable function is to provide σ^E activity. *Mol. Microbiol.* **40:** 1323–1333.

Alba, B.M., Leeds, J.A., Onufryk, C., Lu, C.Z., and Gross, C.A. 2002. DegS and YaeL participate sequentially in the cleavage of RseA to activate the σ^E-dependent extracytoplasmic stress response. *Genes & Dev.* **16:** 2156–2168.

Bashyam, M.D. and Hasnain, S.E. 2004. The extracytoplasmic function σ factors: Role in bacterial pathogenesis. *Infect. Genet. Evol.* **4:** 301–308.

Bohn, C., Collier, J., and Bouloc, P. 2004. Dispensable PDZ domain of *Escherichia coli* YaeL essential protease. *Mol. Microbiol.* **52:** 427–435.

Brown, M.S., Ye, J., Rawson, R.B., and Goldstein, J.L. 2000. Regulated intramembrane proteolysis: A control mechanism conserved from bacteria to humans. *Cell* **100:** 391–398.

Browning, D.F., Whitworth, D.E., and Hodgson, D.A. 2003. Light-induced carotenogenesis in *Myxococcus xanthus*: Functional characterization of the ECF σ factor CarQ and anti σ factor CarR. *Mol. Microbiol.* **48:** 237–251.

Burton, R.E., Baker, T.A., and Sauer, R.T. 2005. Nucleotide-dependent substrate recognition by the AAA+ HslUV protease. *Nat. Struct. Mol. Biol.* **12:** 245–251.

Campbell, E.A., Tupy, J.L., Gruber, T.M., Wang, S., Sharp, M.M., Gross, C.A., and Darst, S.A. 2003. Crystal structure of *Escherichia coli* σ^E with the cytoplasmic domain of its anti-σ RseA. *Mol. Cell* **11:** 1067–1078.

Casadaban, M.J. and Cohen, S.N. 1980. Analysis of gene control signals by DNA fusion and cloning in *Escherichia coli*. *J. Mol. Biol.* **138:** 179–207.

Chen, J.C., Viollier, P.H., and Shapiro, L. 2005. A membrane metalloprotease participates in the sequential degradation of a *Caulobacter* polarity determinant. *Mol. Microbiol.* **55:** 1085–1103.

Cowan, S.W., Garavito, R.M., Jansonius, J.N., Jenkins, J.A., Karlsson, R., Konig, N., Pai, E.F., Pauptit, R.A., Rizkallah, P.J., Rosenbusch, J.P., et al. 1995. The structure of OmpF porin in a tetragonal crystal form. *Structure* **3:** 1041–1050.

Dartigalongue, C., Missiakas, D., and Raina, S. 2001. Characterization of the *Escherichia coli* σ^E regulon. *J. Biol. Chem.* **276:** 20866–20875.

De Las Penas, A., Connolly, L., and Gross, C.A. 1997a. σ^E is an essential σ factor in *Escherichia coli. J. Bacteriol.* **179:** 6862–6864.

De Las Penas, A., Connolly, L., and Gross, C.A. 1997b. The σ^E-mediated response to extracytoplasmic stress in *Escherichia coli* is transduced by RseA and RseB, two negative regulators of σ^E. *Mol. Microbiol.* **24:** 373–385.

Dong, T.C. and Cutting, S.M. 2003. SpoIVB-mediated cleavage of SpoIVFA could provide the intercellular signal to activate processing of Pro-σ^K in *Bacillus subtilis. Mol. Microbiol.* **49:** 1425–1434.

Dougan, D.A., Reid, B.G., Horwich, A.L., and Bukau, B. 2002. ClpS, a substrate modulator of the ClpAP machine. *Mol. Cell* **9:** 673–683.

Farrell, C.M., Grossman, A.D., and Sauer, R.T. 2005. Cytoplasmic degradation of ssrA-tagged proteins. *Mol. Microbiol.* **57:** 1750–1761.

Flynn, J.M., Levchenko, I., Seidel, M., Wickner, S.H., Sauer, R.T., and Baker, T.A. 2001. Overlapping recognition determinants within the ssrA degradation tag allow modulation of proteolysis. *Proc. Natl. Acad. Sci.* **98:** 10584–10589.

Flynn, J.M., Levchenko, I., Sauer, R.T., and Baker, T.A. 2004. Modulating substrate choice: The SspB adaptor delivers a regulator of the extracytoplasmic-stress response to the AAA+ protease ClpXP for degradation. *Genes & Dev.* **18:** 2292–2301.

Goldberg, A.L., Moerschell, R.P., Chung, C.H., and Maurizi, M.R. 1994. ATP-dependent protease La (lon) from *Escherichia coli. Methods Enzymol.* **244:** 350–375.

Gottesman, S., Roche, E., Zhou, Y., and Sauer, R.T. 1998. The ClpXP and ClpAP proteases degrade proteins with carboxy-terminal peptide tails added by the SsrA-tagging system. *Genes & Dev.* **12:** 1338–1347.

Grigorova, I.L., Chaba, R., Zhong, H.J., Alba, B.M., Rhodius, V., Herman, C., and Gross, C.A. 2004. Fine-tuning of the *Escherichia coli* σ^E envelope stress response relies on multiple mechanisms to inhibit signal-independent proteolysis of the transmembrane anti-σ factor, RseA. *Genes & Dev.* **18:** 2686–2697.

Guyer, M.S., Reed, R.R., Steitz, J.A., and Low, K.B. 1981. Identification of a sex-factor-affinity site in *E. coli* as γδ. *Cold Spring Harb. Symp. Quant. Biol.* **45:** 135–140.

Herman, C., Prakash, S., Lu, C.Z., Matouschek, A., and Gross, C.A. 2003. Lack of a robust unfoldase activity confers a unique level of substrate specificity to the universal AAA protease FtsH. *Mol. Cell* **11:** 659–669.

Hiratsu, K., Amemura, M., Nashimoto, H., Shinagawa, H., and Makino, K. 1995. The *rpoE* gene of *Escherichia coli*, which encodes σ^E, is essential for bacterial growth at high temperature. *J. Bacteriol.* **177:** 2918–2922.

Jensen, K.F. 1993. The *Escherichia coli* K-12 'wild types' W3110 and MG1655 have an *rph* frameshift mutation that leads to pyrimidine starvation due to low *pyrE* expression levels. *J. Bacteriol.* **175:** 3401–3407.

Kanehara, K., Ito, K., and Akiyama, Y. 2002. YaeL (EcfE) activates the σ^E pathway of stress response through a site-2 cleavage of anti-σ^E, RseA. *Genes & Dev.* **16:** 2147–2155.

Kanehara, K., Ito, K., and Akiyama, Y. 2003. YaeL proteolysis of RseA is controlled by the PDZ domain of YaeL and a Gln-rich region of RseA. *EMBO J.* **22:** 6389–6398.

Kim, Y.I., Burton, R.E., Burton, B.M., Sauer, R.T., and Baker, T.A. 2000. Dynamics of substrate denaturation and translocation by the ClpXP degradation machine. *Mol. Cell* **5:** 639–648.

Levchenko, I., Yamauchi, M., and Baker, T.A. 1997. ClpX and MuB interact with overlapping regions of Mu transposase: Implications for control of the transposition pathway. *Genes & Dev.* **11:** 1561–1572.

Levchenko, I., Grant, R.A., Flynn, J.M., Sauer, R.T., and Baker, T.A. 2005. Versatile modes of peptide recognition by the AAA+ adaptor protein SspB. *Nat. Struct. Mol. Biol.* **12:** 520–525.

Matson, J.S. and DiRita, V.J. 2005. Degradation of the membrane-localized virulence activator TcpP by the YaeL protease in *Vibrio cholerae. Proc. Natl. Acad. Sci.* **102:** 16403–16408.

Maurizi, M.R., Thompson, M.W., Singh, S.K., and Kim, S.H. 1994. Endopeptidase Clp: ATP-dependent Clp protease from *Escherichia coli. Methods Enzymol.* **244:** 314–331.

Mecsas, J., Rouviere, P.E., Erickson, J.W., Donohue, T.J., and Gross, C.A. 1993. The activity of σ^E, an *Escherichia coli* heat-inducible σ-factor, is modulated by expression of outer membrane proteins. *Genes & Dev.* **7:** 2618–2628.

Miller, J.H. 1972. *Experiments in molecular genetics*. Cold Spring Harbor Laboratory, Cold Spring Harbor, NY.

Missiakas, D. and Raina, S. 1998. The extracytoplasmic function σ factors: Role and regulation. *Mol. Microbiol.* **28:** 1059–1066.

Missiakas, D., Betton, J.M., and Raina, S. 1996. New components of protein folding in extracytoplasmic compartments of *Escherichia coli* SurA, FkpA and Skp/OmpH. *Mol. Microbiol.* **21:** 871–884.

Missiakas, D., Mayer, M.P., Lemaire, M., Georgopoulos, C., and Raina, S. 1997. Modulation of the *Escherichia coli* σ^E (RpoE) heat-shock transcription-factor activity by the RseA, RseB and RseC proteins. *Mol. Microbiol.* **24:** 355–371.

Nikaido, H. 1996. Outer membrane. In Escherichia coli *and* Salmonella*: Cellular and molecular biology* (eds. F.C. Neidhardt et al.), pp. 29–47. ASM Press, Washington, DC.

Raina, S., Missiakas, D., and Georgopoulos, C. 1995. The *rpoE* gene encoding the σ^E (σ^{24}) heat shock σ factor of *Escherichia coli. EMBO J.* **14:** 1043–1055.

Raivio, T.L. and Silhavy, T.J. 2001. Periplasmic stress and ECF σ factors. *Annu. Rev. Microbiol.* **55:** 591–624.

Reiling, S.A., Jansen, J.A., Henley, B.J., Singh, S., Chattin, C., Chandler, M., and Rowen, D.W. 2005. Prc protease promotes mucoidy in *mucA* mutants of *Pseudomonas aeruginosa. Microbiology* **151:** 2251–2261.

Resnekov, O. and Losick, R. 1998. Negative regulation of the proteolytic activation of a developmental transcription factor in *Bacillus subtilis. Proc. Natl. Acad. Sci.* **95:** 3162–3167.

Rezuchova, B., Miticka, H., Homerova, D., Roberts, M., and Kormanec, J. 2003. New members of the *Escherichia coli* σ^E regulon identified by a two-plasmid system. *FEMS Microbiol. Lett.* **225:** 1–7.

Rhodius, V.A., Suh, W.C., Nonaka, G., West, J., and Gross, C.A. 2006. Conserved and variable functions of the σ^E stress response in related genomes. *PLoS Biol.* **4:** 43–59.

Rouviere, P.E. and Gross, C.A. 1996. SurA, a periplasmic protein with peptidyl-prolyl isomerase activity, participates in the assembly of outer membrane porins. *Genes & Dev.* **10:** 3170–3182.

Rouviere, P.E., De Las Penas, A., Mecsas, J., Lu, C.Z., Rudd, K.E., and Gross, C.A. 1995. *rpoE*, the gene encoding the second heat-shock σ factor, σ^E, in *Escherichia coli. EMBO J.* **14:**

1032–1042.
Sambrook, J., Fritsch, E.F., and Maniatis, T. 1989. *Molecular cloning. A laboratory manual*. Cold Spring Harbor Laboratory Press, Cold Spring Harbor, NY.
Schobel, S., Zellmeier, S., Schumann, W., and Wiegert, T. 2004. The *Bacillus subtilis* σ^W anti-σ factor RsiW is degraded by intramembrane proteolysis through YluC. *Mol. Microbiol.* **52:** 1091–1105.
Schweder, T., Lee, K.H., Lomovskaya, O., and Matin, A. 1996. Regulation of *Escherichia coli* starvation σ factor (σ^S) by ClpXP protease. *J. Bacteriol.* **178:** 470–476.
Studier, F.W. and Moffatt, B.A. 1986. Use of bacteriophage T7 RNA polymerase to direct selective high-level expression of cloned genes. *J. Mol. Biol.* **189:** 113–130.
Walsh, N.P., Alba, B.M., Bose, B., Gross, C.A., and Sauer, R.T. 2003. OMP Peptide signals initiate the envelope-stress response by activating DegS protease via relief of inhibition mediated by its PDZ domain. *Cell* **113:** 61–71.
Weihofen, A. and Martoglio, B. 2003. Intramembrane-cleaving proteases: Controlled liberation of proteins and bioactive peptides. *Trends Cell Biol.* **13:** 71–78.
Wilken, C., Kitzing, K., Kurzbauer, R., Ehrmann, M., and Clausen, T. 2004. Crystal structure of the DegS stress sensor: How a PDZ domain recognizes misfolded protein and activates a protease. *Cell* **117:** 483–494.
Zhou, R. and Kroos, L. 2004. BofA protein inhibits intramembrane proteolysis of pro-σ^K in an intercompartmental signaling pathway during *Bacillus subtilis* sporulation. *Proc. Natl. Acad. Sci.* **101:** 6385–6390.
Zhou, R. and Kroos, L. 2005. Serine proteases from two cell types target different components of a complex that governs regulated intramembrane proteolysis of pro-σ^K during *Bacillus subtilis* development. *Mol. Microbiol.* **58:** 835–846.